Journal of Magnetics 15(4), 149-154 (2010) DOI: 10.4283/JMAG.2010.15.4.149

Numerical Study on Current-Induced Switching of Synthetic Antiferromagnet

Seo-Won Lee and Kyung-Jin Lee*

Department of Materials Science and Engineering, Korea University, Seoul 136-713, Korea

(Received 20 October 2010, Received in final form 24 November 2010, Accepted 25 November 2010)

Synthetic antiferromagnets (SAFs) are used as free layer structures for various magnetic devices utilizing spin-transfer torque (STT). Therefore, it is important to understand current-induced excitation of SAFs. By means of drift-diffusion and macrospin models, we studied the current-induced excitation of a SAF-free layer structure (NiFe/Ru/NiFe). The simulation results were compared with the previous experimental results [N. Smith *et al*., Phys. Rev. Lett. 101, 247205 (2008)]. We confirmed that a nonzero STT through the Ru layer is essential for explaining the experimental results.

Keywords : spin transfer torque, synthetic antiferromagnet

1. Introduction

An electric current spin-polarized by a ferromagnet (FM) transfers its spin angular momentum to the local magnetization of another FM, *i.e.*, spin-transfer torque (STT) [1]. STT can fully reverse the magnetization in a zero or low external magnetic field [2], whereas it can induce the steady precession motion of magnetization in high magnetic fields [3]. From the application point of view, current-induced magnetization switching and precession motion is applicable to magnetic memory devices and tunable microwave oscillator devices, respectively. Owing to the potential for these applications and interesting physics, STT has been extensively studied for over a decade.

Until now, most of the experimental and theoretical studies on STT have been performed on planar spin valve structures of the type polarizer/spacer/free layer, where the polarizer and free layer consist of a single in-plane magnetized FM. Recently, a synthetic antiferromagnet (SAF), consisting of two FMs antiferromagnetically coupled via a Rudrman-Kittel-Kasuya-Yosida (RKKY) interaction across a thin Ru layer, has been used instead of a single free layer to achieve lower switching current density and an intense microwave emission peak [4,5]. Thus, it is important to study STT and STT-induced magnetization dynamics in SAF for design and analysis of experiments including SAF-free layer structures.

For a structure including three or more FMs, the STT exerted on a FM is influenced by local magnetization of not only the neighbor FMs but also by other FMs because the spin accumulation related to the STT at a local point is affected by the magnetization configuration in the overall structure [6]. Thus, it is essential to consider the variation of the STT with respect to the magnetization configuration in a structure containing a SAF-free layer which consists of three or more FMs. In the experimental results the SAF-free layer testing (SAF-pinned layer/Cu/SAF-free layer) [7], however, two main assumptions for the STT were employed in interpreting the results. Firstly, the angular dependence of STT at each interface was ignored and, secondly, the polarization factor which is a parameter for STT was overestimated at the interface of Ru. In this study, we consider the angular dependence of STT and simulate the magnetization dynamics of the SAF-free layer. By considering the effect of angular dependence of STT through not only the Cu layer but also the Ru layer, we found that the STT could be important for the current-induced magnetization dynamics of the FMs. Also, the experimental results in Ref. [7] could be explained by our model calculation without an overestimated polarization factor.

2. Models and Description

The structure used in the calculation is PtMn(7)|PL(3)|Ru(0.7)|RL(3)|Cu(4)|FM1(t_{FM2}+4)|Ru(0.7)|FM2(t_{FM2})|Cu

*Corresponding author: Tel: +82-2-3290-3289
Fax: +82-2-928-3584, e-mail: kj_lee@korea.ac.kr

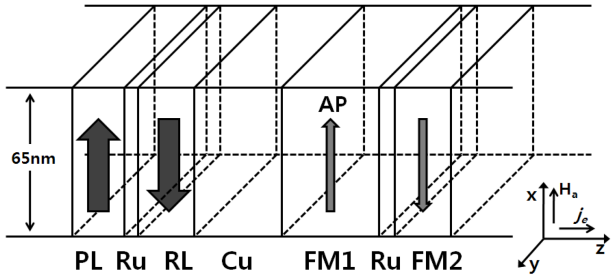

Fig. 1. Schematic structure used in the calculation.

(infinite) (all in *nanometers*), as depicted in Fig. 1. The pinned layer (PL, CoFe), which is fixed by the anti-ferromagnetic material (AFM, PtMn), and the reference layer (RL, CoFe), which is anti-ferromagnetically coupled with PL, make up a SAF-pinned layer. The SAF-free layer is composed of FM1 and FM2 (both NiFe) and is assumed to be patterned into 150 × 50 nm^2. In this structure, STTs are exerted on three interfaces, that is, Cu|FM1 (interface 1), FM1|Ru(interface 2), and Ru|FM2(interface 3). As shown in Fig. 1, when the electrons flow along the +z-axis, the current is positive and a positive magnetic field is applied along the +x-axis. We indicate that, for the AP-state of magnetization, the magnetization of FM1 is aligned anti-parallel to the RL and the FM2 is aligned parallel to the RL while we indicate that, for the initial P-state, the FM1 is parallel to RL and FM2 is anti-parallel to RL.

We simulated the magnetization dynamics of FM1 and FM2 within a macrospin assumption by using the LLG equation that included the STT-term, as shown below,

$$\frac{\partial \mathbf{m}_i}{\partial t} = -\gamma_g \mathbf{m}_i \times \mathbf{H}_{eff} + \alpha \mathbf{m}_i \times \frac{\partial \mathbf{m}_i}{\partial t} + \mathrm{STT}_{\mathrm{FM}i}, \qquad (1)$$

where $\mathbf{m}_i$ is the normalized magnetization of FMi, γ_g is the gyromagnetic ratio, α is the Gilbert damping constant, $\mathbf{H}_{eff}$ is the effective magnetic field including the demagnetization field, dipolar coupling field, RKKY-exchange field, and applied external field. In this study, $\mathrm{STT}_{\mathrm{FM}i}$ includes only in-plane STT because the out-of-plane STT in metallic multilayers is negligible [8], while that in magnetic tunnel junctions is non-negligible [9]. The first and the second terms in eq. (1) correspond to precession and damping motion of magnetization, respectively. The third term, $\mathrm{STT}_{\mathrm{FM}i}$ exerted on FMi is described as follows,

$$\begin{aligned}\mathrm{STT}_{\mathrm{FM1}} &= \mathrm{STT}_1 + \mathrm{STT}_2 \\ &= \gamma_g [a_{J1}\mathbf{m}_1 \times (\mathbf{m}_1 \times \mathbf{p}) + a_{J2}\mathbf{m}_1 \times (\mathbf{m}_1 \times \mathbf{m}_2)], \\ \mathrm{STT}_{\mathrm{FM2}} &= \gamma_g [a_{J3}\mathbf{m}_2 \times (\mathbf{m}_2 \times \mathbf{m}_1)], \end{aligned} \qquad (2)$$

where STT_i is the STT exerted on interface i, a_{Ji} is an amplitude of the in-plane STT at interface i, and $\mathbf{p}$ is unit vector of magnetization of RL. As shown in the above equation, the STT exerted on each FM is determined by the magnetization directions, $\mathbf{m}_1$, $\mathbf{m}_2$, and $\mathbf{p}$. Also, because the amplitude of STT at each interface, a_{Ji}, is determined by the overall magnetization configuration according to the drift-diffusion theory [10], the STT on each FM could be quite complicated with the many magnetizations of the FMs. From the drift-diffusion model, the polarization factor determining the amplitude of STT in the form of $a_{Ji}(\theta_1, \theta_2) = (\hbar/2e)(J_e/M_{Si}t_i)\cdot\eta_i(\theta_1, \theta_2)$ is given by

$$\begin{aligned}\eta_1 &= -\frac{\hbar}{e^2}\left[\mathrm{Re}\{G_{\uparrow\downarrow}\}_{\mathrm{Cu}}(g_y\cot\theta_1 + g_x) + \mathrm{Im}\{G_{\uparrow\downarrow}\}_{\mathrm{Cu}}\frac{g_z}{\sin\theta_1}\right]_{\text{interface 1}} \\ \eta_2 &= -\frac{\hbar}{e^2}\left[\mathrm{Re}\{G_{\uparrow\downarrow}\}_{\mathrm{Ru}}(g_y\cot(\theta_1-\theta_2) + g_x) \right. \\ &\qquad \left. + \mathrm{Im}\{G_{\uparrow\downarrow}\}_{\mathrm{Ru}}\frac{g_z}{\sin(\theta_1-\theta_2)}\right]_{\text{interface 2}}, \\ \eta_3 &= -\frac{\hbar}{e^2}\left[\mathrm{Re}\{G_{\uparrow\downarrow}\}_{\mathrm{Ru}}(g_y\cot(\theta_2-\theta_1) + g_x) \right. \\ &\qquad \left. + \mathrm{Im}\{G_{\uparrow\downarrow}\}_{\mathrm{Ru}}\frac{g_z}{\sin(\theta_2-\theta_1)}\right]_{\text{interface 3}}, \end{aligned} \qquad (3)$$

where M_{Si} is the saturation magnetization of FMi, t_i is the thickness of FMi, J_e is the current density, θ_1 and θ_2 are

Table 1. Spin transport parameters used in our calculation.

Material	Measured resistivity ($\mu\Omega\cdot$cm)	Bulk scattering asymmetry β	Measured RA (m$\Omega\cdot\mu$m^2)	Interfacial scattering asymmetry γ	Spin flip length (nm)	Spin memory loss (%)
PtMn [13]	180.0	0.0			2.0	
CoFe [14]	20.0	0.6			15.0	
Ru [15]	20.0	0.0			12.0	
Cu [16]	5.0	0.0			200.0	
NiFe [16]	25.0	0.7			4.5	
PtMn/CoFe [13]			0.5	0.1		63.2 (unknown)
CoFe/Ru [15]			0.5	–0.2		31.0
CoFe/Cu [13]			1.0	0.7		33.0 (unknown)
NiFe/Cu [16]			0.2	0.6		33.0
NiFe/Ru			0.5 (unknown)	–0.2 (unknown)		28.3 (unknown)

angles of magnetization of FM1 and FM2, respectively, tilting from RL, $G_{\uparrow\downarrow}$ is the spin mixing conductance, and **g** is the spin accumulation. Because the imaginary part of spin mixing conductance is much smaller than the real part, it is ignored in our calculation. Spin accumulation could be obtained by considering the spin transport parameters and the thicknesses of layers, and thus the polarization factor changes with not only the angle of the FMs, but also with the layers in the structure. Most of the spin transport parameters used in the calculation were taken from the literature and are listed in Table 1. The unknown values for some materials are assumed to be moderate. The polarization factor is dependent on the magnetization angles and thicknesses of FMs in our calculation because the material is not altered (PL and RL are CoFe and FM1 and FM2 are NiFe).

3. Results and Discussion

3.1. Angular dependence of STT

STT_i is basically proportioned to $\sin\theta$ due to its cross product with neighboring magnetizations where θ is the angle between two magnetizations. However, because the amplitude of STT_i, a_{Ji}, is not a constant, rather it is severely dependent on the magnetization configuration of the overall structure, it exhibits complicated angular dependence on STT_i. The variation of STTs at three interfaces is shown in two cases. In the first case, the STT through Ru (STT_2 and STT_3) is ignored with zero $\mathrm{Re}\{G_{\uparrow\downarrow}\}_{\mathrm{Ru}}$ (Fig. 2(a)) and in the second case, it is considered with non-zero $\mathrm{Re}\{G_{\uparrow\downarrow}\}_{\mathrm{Ru}}$ (Fig. 2(b) STT_1, (c) STT_2, (d) STT_3). The thicknesses of FM1 and FM2 are fixed as 6 and 2 *nm*. For the first case, STT_1 is mainly dependent on the θ_1(angle 1), but it also slightly changes with θ_2(angle 2) due to variation of the spin accumulation. For the second case, $\mathrm{Re}\{G_{\uparrow\downarrow}\}_{\mathrm{Ru}}$ is assumed to be equal to $\mathrm{Re}\{G_{\uparrow\downarrow}\}_{\mathrm{Cu}}$. In Fig. 2(b), the variation of STT_1 with θ_2 is less than that for the first case in Fig. 2(a). This indicates that $\mathrm{Re}\{G_{\uparrow\downarrow}\}_{\mathrm{Ru}}$ affects spin accumulation in the overall structure. In the drift-diffusion model, all parameters, such as spin mixing conductance, spin asymmetry factor, and resistance, have effects on the spin accumulation and spin current. In Fig. 2(c) and 2(d), angular dependence of STTs through Ru the layer is complex because it is directly influenced by both of the FM1 and FM2 angles.

3.2. Critical current

To understand the effect of angle-dependent STT through Ru on the excitation of the SAF-free layer, the critical currents (I_c) for excitation of FM1 and FM2 are obtained

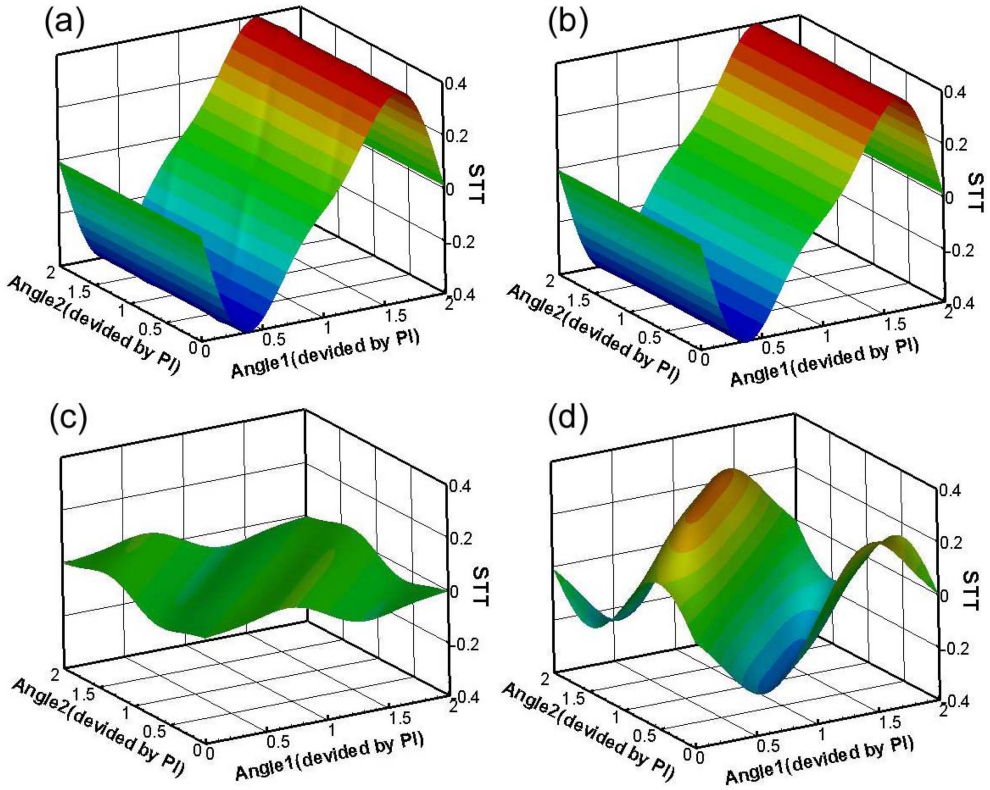

Fig. 2. STTs when r is (a) 0 and (b~d) 1; r indicates the ratio of $\mathrm{Re}\{G_{\uparrow\downarrow}\}_{\mathrm{Ru}}$ to $\mathrm{Re}\{G_{\uparrow\downarrow}\}_{\mathrm{Cu}}$. (a) and (b) show the STTs at the interface of Cu|FM1 (interface 1) and (c) and (d) are for STTs at FM1|Ru (interface 2) and Ru|FM2 (interface 2), respectively.

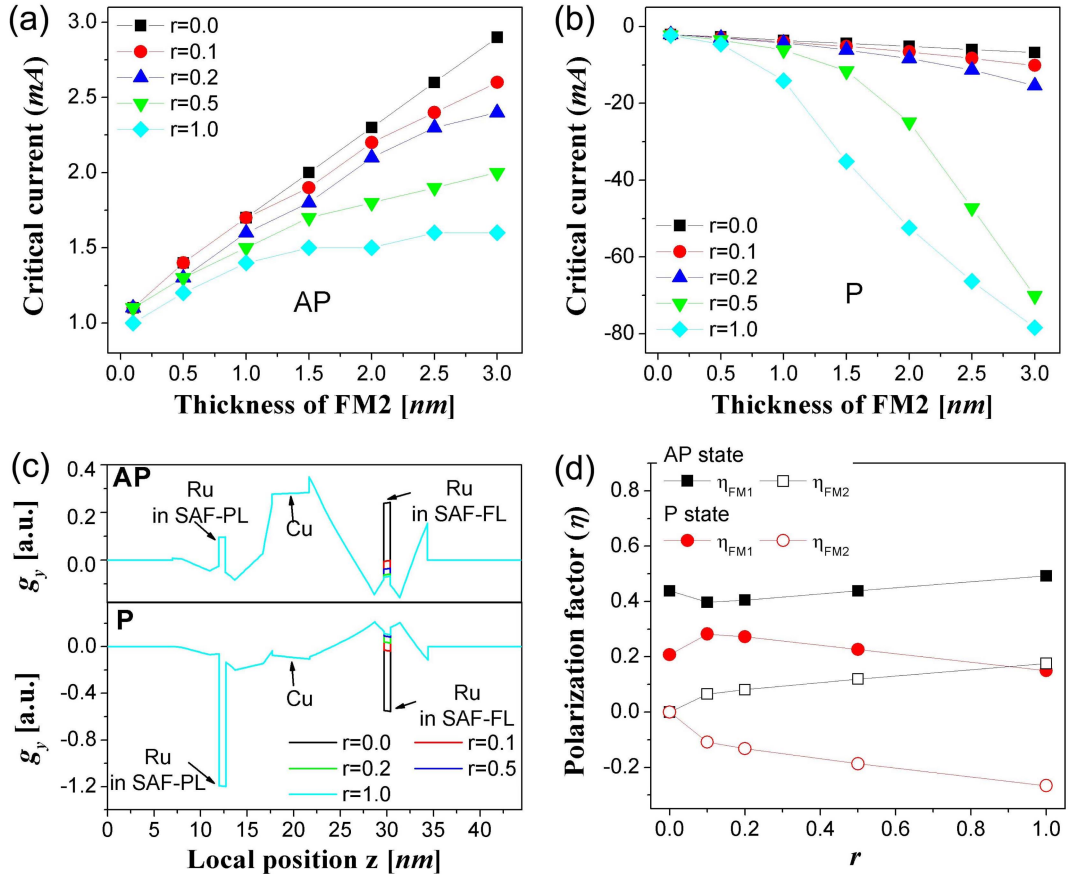

Fig. 3. Critical current with thickness of FM2 for (a) the initial AP-state and (b) the initial P-state. (c) The transverse component of spin accumulation at every local position in the structure with various r values. (d) The polarization factors for FM1 and FM2 at both the AP- and P-state as a function of r.

with various r values (ratio of $\mathrm{Re}\{G_{\uparrow\downarrow}\}_{\mathrm{Ru}}$ to $\mathrm{Re}\{G_{\uparrow\downarrow}\}_{\mathrm{Cu}}$). We vary $\mathrm{Re}\{G_{\uparrow\downarrow}\}_{\mathrm{Ru}}$ due to its unknown value but it would be obtained by such an ab-initio calculation [11]. Firstly, we calculated the polarization factor at each interface with various r values as described in part A, and secondly, we simulated magnetization dynamics including an angle-dependent polarization factor for 100 ns. If the current perpendicular to the plane is applied, the magnetization is excited due to an in-plane STT at the critical current. This is shown in Fig. 3(a) for the initial AP-state and 3(b) for the initial P-state with increasing thicknesses of FM2, which indicates concurrent change of thickness of FM1 ($t_{\mathrm{FM1}} = t_{\mathrm{FM2}} + 4$ *nm*). For the initial AP-state, the SAF-free layer is excited for $\mathrm{I} > 0$, whereas for the initial P-state, it is excited for $\mathrm{I} < 0$. To insure the initial states and to reproduce the experimental conditions in Ref. [7], an external field (H_a) was applied (+600 *Oe* for AP-state and –600 *Oe* for P-state). In Fig. 3(a), we could find that the critical current increases for both AP- and P-states as the thickness of the SAF-free layer increases. This is reasonable because the critical current is in proportion to the thickness of the FM by relation of $I_c \sim (\alpha/h)M_s t(H_K + 2pM_s)$, where H_K is the anisotropy field [12]. Also, the critical current for the AP-state is smaller than that for the P-state, even for a zero r. This could be interpreted with the polarization factor, which is larger for the AP-state. This originated from the spin accumulation in the normal metal shown in (Fig. 3(c)). The polarization factor for the AP-state is three times of that for the P-state when r is zero, as shown in Fig. 3(d).

As r increases from 0 to 1, $|I_c^{\mathrm{AP}}|$ decreases but $|I_c^{\mathrm{P}}|$ greatly increases. This is explained by the change of the transverse component of spin accumulation (g_y) in the Ru layer as $\mathrm{Re}\{G_{\uparrow\downarrow}\}_{\mathrm{Ru}}$ increases (Fig. 3(c)). This causes the modification of the polarization factor at interfaces 2 and 3, as shown in Fig. 3(d), and this substantially influences the critical current. In Fig. 3(c) and (d), the thicknesses of FM1 and FM2 are fixed at 6 and 2 *nm*, respectively. In Fig. 3(d), η_{FM1} is the polarization factor for FM1 that includes η_1 and η_2, and similarly, η_{FM2} is the polarization

factor for FM2 that includes η_3. Positive η_{FM1} and η_{FM2} cause the excitation of FM1 and FM2, while negative η_{FM1} and η_{FM2} cause the stabilization of them. In the AP-state, η_{FM1} and η_{FM2}, which are larger than those of the P-state, mostly increase with r. This induces the decrease of I_c^{AP} while increasing r. However, for the initial P-state, h_{FM1}, which is positive but smaller than that of the AP-state, diminishes with r, and η_{FM2} is even negative, which stabilizes FM2. As a result, FM1 is less excited and FM2 is more stabilized as r increases. This leads to a significant decrease of the critical current for the initial P-state.

Since the critical currents for the initial AP- and P-states are considerably affected by r, the unknown $\mathrm{Re}\{G_{\uparrow\downarrow}\}_{Ru}$ could be estimated by comparing I_c^{AP} and I_c^{P} from our calculation with the experimental results. However, it is inappropriate to directly compare the values of I_c^{AP} and I_c^{P} because they are dependent on the damping constant, saturation magnetization, and anisotropy constant, which are experimentally changeable parameters. Rather, it is valid to compare I_c^{AP}/I_c^{P} or I_c^{P}/I_c^{AP} which are only related to η^{P}/η^{AP} or η^{AP}/η^{P} owing to the eliminated experimental parameters. In Fig. 4, the experimentally obtained values of I_c^{P}/I_c^{AP} by N. Smith *et al.* [7] are depicted as open squares. The calculated ones are shown in dotted line and solid lines with different r value. If r is 0 and $\eta^{AP}{}_1$ and $\eta^{P}{}_1$ are fixed at 0.75 and 0.25 (dotted line), where angular dependence of STT is simply estimated with fixed $\eta^{AP}{}_1$ and $\eta^{P}{}_1$, I_c^{P}/I_c^{AP} remains around 3 because $\eta^{AP}{}_1/\eta^{P}{}_1$ is 3. However, if the angular dependence of STT is fully considered, I_c^{P}/I_c^{AP} increases with thickness of FM even if

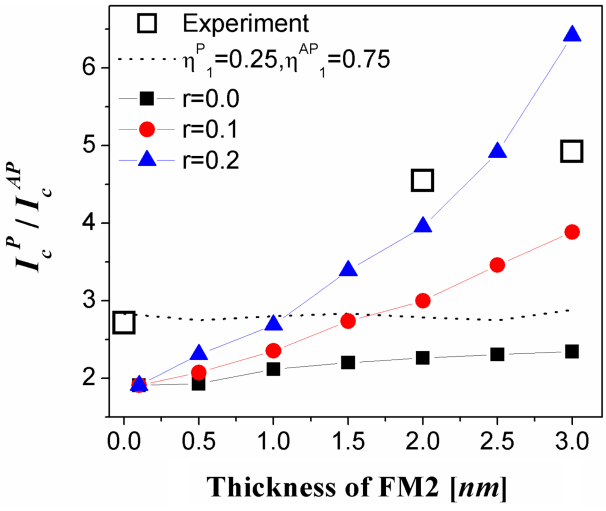

Fig. 4. I_c^{P}/I_c^{AP} values from experimental results (open square) and calculated results (dotted line and solid symbols). For dotted line, r is 0 and $\eta^{AP}{}_1$ and $\eta^{P}{}_1$ are fixed at 0.75 and 0.25. For solid symbols, the angular dependence of STT is fully considered with various r values.

r is 0. This is because we obtained the angular dependence of STT for each thickness of FM. Where r is 0.1 and 0.2, I_c^{P}/I_c^{AP} severely increases with thickness and it exhibits similar slope with experimental results (open square). However, one cannot find r values at which I_c^{P}/I_c^{AP} perfectly agree with the experimental one. This deviation is caused by a few unknown spin transport parameters. The angle-dependent STT calculated by the drift-diffusion model seriously changes with the spin transport parameters and it should be obtained by CPP-GMR experiment.

4. Conclusion

In studying magnetization dynamics of a SAF-free layer, the STT through Ru was ignored or overestimated in other previous papers. In this work, while considering a non-zero spin mixing conductance at the interface of Ru, we investigated the effect of STT through Ru on the magnetization dynamics of a SAF-free layer. The STT through not only Cu, but also Ru, was obtained by the extended drift-diffusion model. Considering angle-dependent STT, we found that the STT considerably affects the magnetic excitation of the SAF-free layer. Also, when the spin mixing conductance of Ru is in the range of 10% to 20% of that of Cu, I_c^{P}/I_c^{AP} roughly agrees with the experimental results.

Acknowledgement

This work was supported by the Fundamental R&D Program for Core Technology of Materials funded by the Ministry of Commerce, Industry and Energy, Republic of Korea, and the DRC Program funded by KRCF.

References

[1] J. C. Slonczewski, J. Magn. Magn. Mater. **159**, L1 (1996); L. Berger, Phys. Rev. B **54**, 9353 (1996).
[2] E. B. Myers *et al.*, Science **285**, 867 (1999); J. A. Katine *et al.*, Phys. Rev. Lett. **84**, 3149 (2000); A. Yamaguchi *et al.*, Phys. Rev. Lett. **92**, 077205 (2004).
[3] G. Tatara *et al.*, J. Phys. Soc. Jpn. **76**, 054707 (2007); S.-W. Jung *et al.*, Appl. Phys. Lett. **92**, 202508 (2008); V. Vlaminck and M. Bailleul, Science **322**, 410 (2008); S.-M. Seo *et al.*, Phys. Rev. Lett. **102**, 147202 (2009).
[4] J. Hayakawa *et al.*, Jap. J. Appl. Phys. **45**, L1057 (2006); T. Ochiai *et al.*, Appl. Phys. Lett. **86**, 242506 (2005); J. Hayakawa *et al.*, IEEE Trans. Magn. **44**, 1962 (2008); M. Ichimura *et al.*, J. Appl. Phys. **105**, 07D120 (2009); C. -T. Yen *et al.*, Appl. Phys. Lett. **93**, 092504 (2008); X. Yao *et al.*, IEEE Trans. Magn. **44**, 2496 (2008); K. Lee *et*

al., J. Appl. Phys. **106**, 024513 (2009); C.-Y. You, J. Appl. Phys. **107**, 073911 (2010); C.-Y. You, Curr. Appl. Phys. **10**, 952 (2010).

[5] S. Ikeda *et al*., IEEE Trans. Electron Devices **54**, 991 (2007); D. Gussakova *et al*., Phys. Rev. B **79**, 104406 (2009).

[6] P. Balaz, M. Gmitra, and J. Barnaœ, Phys. Rev. B. **80**, 174404 (2009).

[7] N. Smith, S. Maat, M. J. Carey, and J. R. Childress, Phys. Rev. Lett. **101**, 247205 (2008).

[8] J. C. Sankey, Y.-T. Cui, J. Z. Sun, J. C. Slonczewski, R. A. Buhrman, and D. C. Ralph, Nature Phys. **4**, 67 (2008).

[9] H. Kubota *et al*., Nature Phys. **4**, 37 (2008); S.-C. Oh *et al*., Nature Phys. **5**, 898 (2009); K. J. Lee *et al*., Nature Mater. **3**, 877 (2004).

[10] A. Brataas *et al*., Phys. Rev. Lett. **84**, 2481 (2000); A. Brataas *et al*., Eur. Phys. J. B **22**, 99 (2001); J. Barnaœ *et al*., Phys. Rev. B **72**, 024426 (2005); S. W. Lee and K. J. Lee, J. Kor. Phys. Soc. **55**, 1501 (2009).

[11] M. Zwierzycki, Y. Tserkovnyak, P. J. Kelly, A. Brataas, and G. E. W. Bauer, Phys. Rev. B **71**, 064420 (2005).

[12] J. Grollier, V. Cros, H. Jaffres, A. Hamzim, J. M. George, G. Faini, J. B. Youssef, H. L Gall, and A. Fert, Phys. Rev. B **67**, 174402 (2003).

[13] N. Strelkov and A. Vedyaev, and B. Dieny, J. Appl. Phys. **94**, 3278 (2003).

[14] H. Yuasa, M. Yoshikawa, Y. Kamiguchi, K. Koi, H. Iwasaki, M. Takagishi, and M. Sahashi, J. Appl. Phys. **92**, 2646 (2002).

[15] K. Eid, R. Fonck, M. AlHajDarwish, W. P. Pratt Jr., and J. Bass, J. Appl. Phys. **91**, 8102 (2002).

[16] K. Eid, W. P. Pratt Jr., and J. Bass, J. Appl. Phys. **93**, 3445 (2003).